Available online at www.sciencedirect.com
ScienceDirect
Int. J. Electron. Commun. (AEÜ) 62 (2008) 483–489
International Journal AEÜ of Electronics and Communications
www.elsevier.de/aeue

Design of distributed-element RF filters via reflectance data modeling

Metin Şengül[a,*], Sıddık B. Yarman[b], Christian Volmer[c], Matthias Hein[c]

[a] *Institute for Information Technology, Technische Universität Ilmenau, 98684 Ilmenau, Germany*
[b] *İstanbul University, Engineering Faculty, 34320 Avcılar-İstanbul, Turkey*
[c] *Institute for Information Technology, Technische Universität Ilmenau, 98684 Ilmenau, Germany*

Received 25 September 2006; accepted 23 May 2007

Abstract

A reflectance-based modeling method is presented, to obtain the distributed-element counterpart of a lumped-element network, which is described by measured or computed reflectance data at a set of frequencies. Numerical generation of the scattering parameters forms the basis of this modeling tool. It is not necessary to select a circuit topology for the distributed-element model, which is the natural consequence of the modeling process. Our approach supplements the known interpolation methods by a simple technique that does not involve complicated cascaded circuit topologies and whose numerical convergence is proven. To illustrate the utilization of the proposed method, a lumped-element low-pass Chebyshev filter is transformed to its distributed-element counterpart. The filter, designed for a frequency band around 1 GHz, was fabricated and experimentally characterized. We find excellent agreement between measured and simulated transducer power gain over the entire frequency band.

Keywords: Modeling; Distributed-element networks; Filters

1. Introduction

For many communications engineering applications, circuit models are inevitable. In the literature, the common exercise to model a set of given data starts with the choice of an appropriate circuit topology. In a next step, the element values of the chosen topology are determined, to fit the given data by means of an optimization algorithm. Although this approach is straightforward, it presents serious difficulties: First, the optimization is strongly nonlinear in terms of the element values that may result in local minima or even may prevent convergence. Secondly, there is no established process to initialize the element values of the chosen circuit topology. Worst of all, *the optimum model topology, which describes the physical device optimally, is not known*.

On the other hand, circuit models can be obtained by interpolation techniques [1–3]. For instance in [3], a set of positive real (PR) impedance data were specified in the complex parameter plane, and unambiguous conditions to generate such PR functions were stated. The data were interpolated, step by step, by the formation of cascade blocks. Depending on the nature of the data, a cascade block can be composed of a Foster section, Brune C-type or Brune D-type sections, or a Richards section. The use of such sections in a cascade block introduces complex transmission zeros and requires gyrators or perfectly coupled coils, which might render the model impractical.

These problems can be overcome by the modeling technique presented in this paper: In this technique, it is neither necessary to select a fixed network topology nor to force

* Corresponding author. Permanent address: Kadir Has University, Engineering Faculty, 34083 Cibali, Fatih-İstanbul, Turkey.
Tel.: +90 212 5336532; fax: +90 212 5335753.
E-mail addresses: msengul@khas.edu.tr (M. Şengül), yarman@istanbul.edu.tr (S.B. Yarman), christian.volmer@tu-ilmenau.de (C. Volmer), matthias.hein@tu-ilmenau.de (M. Hein).

1434-8411/$ - see front matter © 2007 Elsevier GmbH. All rights reserved.
doi:10.1016/j.aeue.2007.05.009

any complicated cascade structure into the model. Transmission zeros are placed as required by the physical nature of the data. The unknown parameters are determined by best fits to the given data via a nonlinear optimization algorithm. Eventually, the driving point function is synthesized. Hence, the desired network topology is obtained as a result of the modeling process. Also, an efficient initialization algorithm for the nonlinear optimization part is presented.

In the following section, a distributed-element two-port is described in terms of its scattering parameters. Subsequently, the modeling algorithm is presented. Finally, the design and experimental verification of a Chebyshev filter with distributed-elements is described, to illustrate the power of the proposed method.

2. Mathematical framework

2.1. Scattering parameters

The modeling problem is defined as the generation of a realizable bounded real (BR) reflectance function $S_{11}(\lambda)$ that gives the best fit to a set of given reflection data $S(\mathrm{j}\omega)$. Eventually, this BR reflectance is synthesized from a lossless Darlington two-port with resistive termination, yielding the desired circuit model (Fig. 1). Here, $\lambda = \Sigma + \mathrm{j}\Omega$ is the conventional Richards variable associated with the equal-length transmission lines, or so-called commensurate transmission lines [4]. In detail, $\lambda = \tanh p\tau$, where $p = \sigma + \mathrm{j}\omega$ is the complex frequency and τ is the commensurate one-way delay of the transmission line. Specifically on the imaginary axis ($\Sigma = 0$), the transformation takes the form ($\lambda = \mathrm{j}\Omega = \mathrm{j}\tan\omega\tau$).

Obviously, the solution for the Darlington representation is not unique. The goal is, therefore, to achieve a reasonable BR reflectance function such that the resulting circuit properly describes the physical behavior of the device with the minimal number of elements.

Let $S(\mathrm{j}\omega_i) = S_R(\omega_i) + \mathrm{j}S_X(\omega_i) = \rho(\omega_i)e^{\mathrm{j}\phi(\omega_i)}$ be the given reflectance data, with $\rho(\omega_i) \leqslant 1$ at all sample frequencies ω_i. Let $\{S_{kl}(\lambda); k, l = 1, 2\}$ designate the scattering parameters of the corresponding distributed-element model that defines the reciprocal, lossless two-port (i.e., the Darlington two-port). For such a two-port, the scattering parameters may be expressed in the Belevitch form as follows [5,6]:

$$S(\lambda) = \begin{bmatrix} S_{11}(\lambda) & S_{12}(\lambda) \\ S_{21}(\lambda) & S_{22}(\lambda) \end{bmatrix} = \frac{1}{g(\lambda)} \begin{bmatrix} h(\lambda) & \mu f(-\lambda) \\ f(\lambda) & -\mu h(-\lambda) \end{bmatrix}, \quad (1)$$

where $\mu = f(-\lambda)/f(\lambda) = \pm 1$. For a lossless two-port with resistive termination, energy conversation requires that

$$S(\lambda)S^{\mathrm{T}}(-\lambda) = I, \quad (2a)$$

where I is the identity matrix and "T" designates the transpose of the matrix. The explicit form of (2a) is known as the Feldtkeller equation and is given by

$$g(\lambda)g(-\lambda) = h(\lambda)h(-\lambda) + f(\lambda)f(-\lambda). \quad (2b)$$

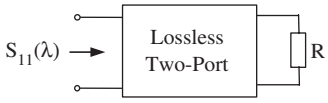

Fig. 1. Darlington representation of the distributed-element model.

In Eqs. (1) and (2b), $g(\lambda)$ is the strictly Hurwitz polynomial of nth degree with real coefficients, and $h(\lambda)$ is a polynomial of nth degree with real coefficients. The polynomial function $f(\lambda)$ includes all transmission zeros of the two-port; its general form is given by

$$f(\lambda) = f_0(\lambda)(1 - \lambda^2)^{n_\lambda/2}, \quad (3)$$

where n_λ specifies the number of equal-length transmission lines contained in the two-port, and $f_0(\lambda)$ is an arbitrary real polynomial. According to Eq. (3), there may be a finite number of transmission zeros in the right half of the λ-plane. Realization of distributed network functions having such factors require, in general, complicated structures like coupled lines, Ikeno-loops, etc., which are difficult to implement and, therefore, undesirable [7,8].

A powerful class of networks contains simple, series or shunt, stubs and equal-length transmission lines only. Series-short stubs and shunt-open stubs produce transmission zeros for $\lambda = \infty$, corresponding to the frequency $\omega = \pi/2\tau$ and odd multiples thereof. Series-open stubs and shunt-short stubs produce transmission zeros for $\lambda = 0$ (i.e., $\omega = 0$). For such networks, the polynomial function $f(\lambda)$ takes the more practical form

$$f(\lambda) = \lambda^k(1 - \lambda^2)^{n_\lambda/2}, \quad (4)$$

where n_λ is the number of equal-length transmission lines in cascade, k is the total number of series-open and shunt-short stubs, and the difference $n - (n_\lambda + k)$ gives the number of series-short and shunt-open stubs. Here, n denotes the degree of the two-port, which is also the degree of $g(\lambda)$. The synthesis of the input impedance, $Z_{in}(\lambda) = (1 + S_{11}(\lambda))/(1 - S_{11}(\lambda))$, for this case, is accomplished by extracting poles at 0 and ∞, corresponding to stubs, while equal-length transmission lines are extracted by employing Richards extraction method [9]. Alternatively, the synthesis can be carried out in a more general fashion using the cascade decomposition technique by Fettweis, which is based on the factorization of transfer matrices [10].

2.2. Rationale of the modeling algorithm

As far as the modeling problem is concerned, one has to generate realizable BR scattering parameters of the lossless two-port of Fig. 1, such that the input reflection coefficient $S_{11}(\lambda)$ fits the given data $S(\mathrm{j}\omega)$: $S_{11}(\mathrm{j}\Omega(\omega)) = S(\mathrm{j}\omega)$ at each

frequency ω_i. This is not an easy task. In the following, a practical modeling algorithm is described which, in addition, guarantees the realizability of the scattering parameters.

From Eq. (1), for a given $\lambda_i = \lambda(\omega_i)$, one can write

$$h(\mathrm{j}\Omega_i) = S(\mathrm{j}\omega_i)g(\mathrm{j}\Omega_i). \tag{5}$$

Eq. (5) indicates that, if the polynomial $g(\mathrm{j}\Omega) = g_R(\Omega) + \mathrm{j}g_X(\Omega)$ is known, the polynomial $h(\mathrm{j}\Omega) = h_R(\Omega) + \mathrm{j}h_X(\Omega)$ can be readily obtained. In fact, this way of thinking constitutes the key point of the proposed modeling method.

In order to determine $g(\mathrm{j}\Omega)$, it should be noted that $|S_{21}(\mathrm{j}\Omega)|^2$ is given on the real frequency axis (namely, $\lambda = 0 + \mathrm{j}\Omega$) by

$$|S_{21}(\mathrm{j}\Omega)|^2 = 1 - \rho^2(\mathrm{j}\omega) = \frac{|f(\mathrm{j}\Omega)|^2}{|g(\mathrm{j}\Omega)|^2}. \tag{6}$$

The numerator polynomial $f(\lambda)$ includes the transmission zeros of the filter to be modeled, with its practical form given by Eq. (4). For given BR reflection coefficients $S(\mathrm{j}\omega)$, one can readily compute the *magnitude* of $g(\mathrm{j}\Omega)$, simply by selecting the form of $f(\mathrm{j}\Omega)$:

$$G(\Omega^2) = |g(\mathrm{j}\Omega)|^2 = g_R^2(\mathrm{j}\Omega) + g_X^2(\mathrm{j}\Omega) = \frac{|f(\mathrm{j}\Omega)|^2}{1 - \rho^2(\mathrm{j}\omega)}, \tag{7}$$

where $G(\Omega^2)$ is an even polynomial in Ω. Hence, Eq. (7) describes a known quantity at each specified frequency. Therefore, the strictly Hurwitz polynomial $g(\lambda)$ can be constructed by means of well established numerical methods [11]. The data points given by Eq. (7) for $|g(\mathrm{j}\Omega)|^2$ describe a polynomial such that

$$G(\Omega^2) = G_0 + G_1\Omega^2 + \cdots + G_n\Omega^{2n} > 0; \quad \forall\Omega. \tag{8}$$

The coefficients $\{G_0, G_1, G_2, \ldots, G_n\}$ can be determined easily by linear or nonlinear interpolation or curve fitting methods. Then, replacing Ω^2 by $-\lambda^2$, the roots of $G(-\lambda^2) = g(\lambda)g(-\lambda)$ can be extracted using explicit factorization techniques, and $g(\lambda)$ constructed from the left half-plane (LHP) roots of $G(-\lambda^2)$ as a strictly Hurwitz polynomial.

Let us describe the linear interpolation of $G(\Omega^2)$. In this regard, selected data points associated with $\sqrt{G(\Omega^2)}$ is expressed in terms of the auxiliary even polynomial $P(\Omega^2) = a_0 + a_1\Omega^2 + \cdots + a_{2(n_d-1)}\Omega^{4(n_d-1)}$ where n_d represents the total number of selected data points to interpolate the polynomial $P(\Omega_j^2) = \sqrt{G(\Omega_j^2)}$; $j = 1, 2, \ldots, n_d$. Thus, coefficients G_j of Eq. (8) are given as $G_0 = a_0^2$ which must be positive; for odd values of j, $G_j = 2\sum_{i=0}^{(i-1)/2} a_i a_{i-j}$; $j = 1, 3, \ldots, \prec 2(n_d - 1)$ for even values of j, $G_j = a_j^2/2 + 2\sum_{i=0}^{i/2} a_i a_{i-j}^2$; $j = 2, 4, \ldots, \prec 2(n_d - 1)$; and finally, $G_{2(n_d-1)} = a_{n_d-1}^2$. It should be noted that in the above interpolation approach, the degree n of the polynomial $G(\Omega^2)$ is set to $n_d - 1$. Details of the linear interpolation algorithm can be found in [11]. As can be seen from the above explanations, positivity of $G(\Omega^2)$ is assured with expense of reducing the degree of freedom in the interpolation process. In return, one neither requires invoking Strum's theorem nor it is necessary to employ nonlinear interpolation techniques to grant the positivness of $G(\Omega^2)$. Hence, computations are drastically simplified.

Once $g(\lambda)$ is generated, $g_R(\mathrm{j}\Omega)$ and $g_X(\mathrm{j}\Omega)$ are computed which, in turn, yield the numerical pair $\{h_R, h_X\}$ by means of Eq. (5). Let $h(\lambda) = \sum_{k=0}^{n} h_k\lambda^k$ designate the numerator polynomial of $S_{11}(\lambda)$ [see Eq. (1)], where $\{h_k; k = 0, 1, 2, \ldots, n\}$ are arbitrary real coefficients. Thus, data points corresponding to the real and the imaginary parts of $h(\mathrm{j}\Omega)$ are given by

$$h_R(\Omega) = \sum_{k=0}^{m} (-1)^k h_{2k}\Omega^{2k} \tag{9a}$$

with $m = n/2$ for n even, and $m = (n-1)/2$ for n odd. Similarly,

$$h_X(\Omega) = \sum_{k=1}^{m} (-1)^{k-1} h_{2k-1}\Omega^{2k-1} \tag{9b}$$

with $m = n/2$ and $m = (n+1)/2$ for even and odd n, respectively.

Putting all pieces together, the unknown real coefficients $\{h_k;\ k = 0, 1, 2, \ldots, n\}$ can be determined by means of straight linear interpolation over the selected frequencies.

It is crucial to point out that $g(\lambda)$, $h(\lambda)$ and $f(\lambda)$ must satisfy the Feldtkeller equation (Eq. (2b)). In this context, the *interpolation via fixed-point iteration* [12] is introduced, which yields consistent triples of $\{g(\lambda), h(\lambda), f(\lambda)\}$ satisfying Eq. (2b).

2.3. Reflection data modeling via fixed-point interpolation

Let us first sketch the fixed-point iteration technique, as described in classical numerical analysis text books such as [13]. Zeros of a nonlinear function $M(X) = F(X) - X$ can be determined using the iterative loop described by

$$X^{(r)} = F(X^{(r-1)}). \tag{10}$$

It is straight forward to prove that, for any initial guess $X^{(0)}$, Eq. (10) converges to the real root $X_{\mathrm{root}} = \lim_{r\to\infty} F(X^{(r)})$ if and only if $|\frac{\mathrm{d}F}{\mathrm{d}X}| < 1$; $\forall X$, where the symbol $|\bullet|$ designates the absolute value.

For the problem under consideration, the polynomial $h(\mathrm{j}\Omega)$ can be determined, point by point, by means of an iterative process employing Eq. (5) over the selected frequencies Ω_i such that

$$h^{(r)}(\mathrm{j}\Omega_i) = S(\mathrm{j}\omega_i)g^{(r-1)}(\mathrm{j}\Omega_i). \tag{11}$$

In this notation, one has to show that $S \cdot g$ describes a function $h = F(h)$ for which $|\frac{\mathrm{d}F}{\mathrm{d}h}| < 1$; $\forall h$. In the following, the iterative process defined by Eq. (11) is described first and then its convergence is proven.

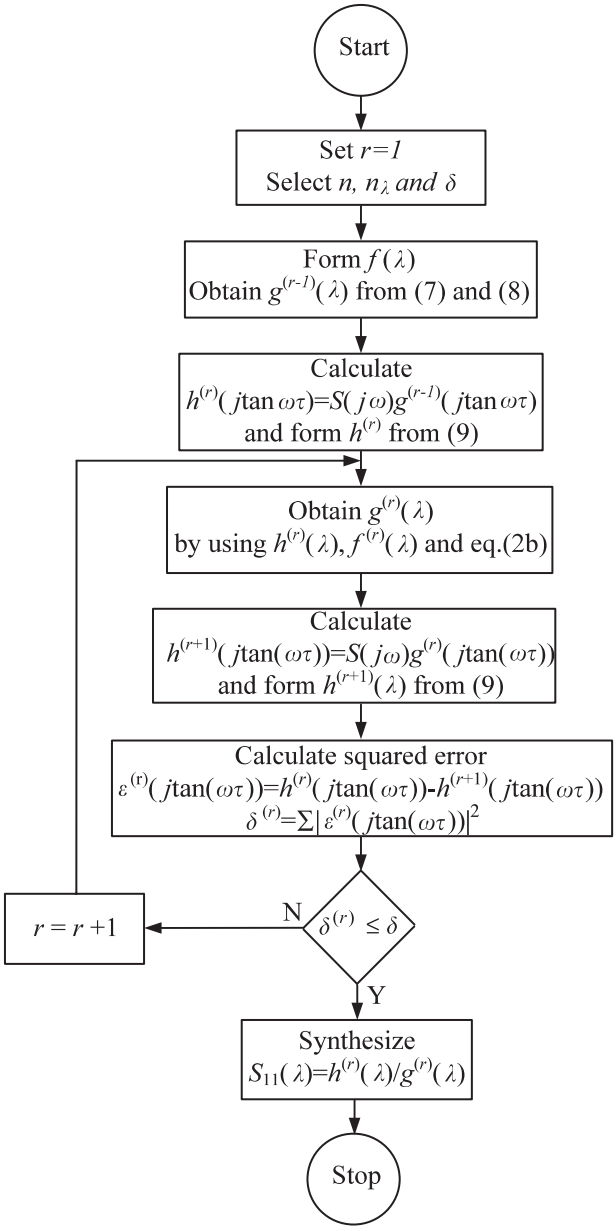

Fig. 2. Flowchart of the modeling algorithm.

Fig. 2 illustrates the logical flow of the iteration loop; the input parameters are summarized in Table 1.

After selecting $f(\lambda)$, $g^{(0)}(\lambda)$ is generated solely in terms of the given data $S(\mathrm{j}\omega_i)$ by explicit factorization of Eq. (8). The first iteration loop is initiated by computing $h^{(1)}(\mathrm{j}\Omega_i) = h_R(\Omega_i) + \mathrm{j}h_X(\Omega_i)$ at the sample frequencies $\{\Omega_i;\ i = 0, 1, 2, \ldots, m\}$. Using Eq. (9), an analytic form of $h^{(1)}(\lambda)$ is obtained by means of a linear interpolation algorithm. Rewriting Eq. (2b) with the help of Eq. (8) leads to

$$\begin{aligned} G^{(1)}(-\lambda^2) &= g^{(1)}(\lambda)g^{(1)}(-\lambda) \\ &= h^{(1)}(\lambda)h^{(1)}(-\lambda) + f(\lambda)f(-\lambda) \\ &= G_0^{(1)} - G_1^{(1)}\lambda^2 + \cdots + (-1)^n G_n^{(1)}\lambda^{2n}, \end{aligned} \tag{12}$$

which allows to generate $g^{(1)}(\lambda)$ from the LHP roots of $G^{(1)}(-\lambda^2)$. Hence, the second iteration loop starts with the computed $g^{(1)}(\mathrm{j}\Omega_i)$, which yield $h^{(2)}(\mathrm{j}\Omega_i)$. Then, $g^{(2)}$ is constructed yielding $h^{(3)}$ and so on. The iteration stops if $|h^{(r)} - h^{(r-1)}| \leqslant \delta$, where $0 < \delta < 1$.

To prove the convergence of the iterative process, it should be noted that the polynomial g can be described in terms of the polynomial h by using Eq. (2b) again:

$$\begin{aligned} g(\mathrm{j}\Omega) &= h(\mathrm{j}\Omega)\frac{h(-\mathrm{j}\Omega)}{g(-\mathrm{j}\Omega)} + f(\mathrm{j}\Omega)\frac{f(-\mathrm{j}\Omega)}{g(-\mathrm{j}\Omega)} \\ &= h(\mathrm{j}\Omega)S_{11}(-\mathrm{j}\Omega) + f(\mathrm{j}\Omega)S_{21}(-\mathrm{j}\Omega). \end{aligned} \tag{13}$$

Inserting Eq. (13) in Eq. (11) one obtains

$$h(\mathrm{j}\Omega) = h(\mathrm{j}\Omega)\rho^2 + S_{11}(\mathrm{j}\Omega)f(\mathrm{j}\Omega)S_{21}(-\mathrm{j}\Omega). \tag{14}$$

The right-hand side of Eq. (14) describes a function F such that $F(h) = h\rho^2 + S_{11}fS_{21}^*$, where "$*$" designates the para-conjugate of the complex valued quantity. Due to the bounded realness, $\mathrm{d}F/\mathrm{d}h = \rho^2 < 1$ holds at all frequencies, except for isolated points where $\rho = 1$. Therefore, the iteration will converge. Clearly, the above process describes contraction mapping yielding the unique solution.

Table 1. Input parameters of the iteration procedure

Input parameter	Explanation
$S(\mathrm{j}\omega_i) = S_R(\omega_i) + \mathrm{j}S_X(\omega_i);\ i = 1, 2, \ldots, m$	Reflectance data given at the sample frequencies ω_i
n	Desired number of distributed elements
n_λ	Desired number of equal-length transmission lines
k	Desired number of series-open and shunt-short stubs
$f(\lambda)$	A polynomial constructed from the transmission zeros
δ	Stopping criterion for the iterative process

3. Application to filter design: an example

In order to illustrate the algorithm described in Section 2, the model was applied to a lumped-element low-pass Chebyshev filter. In this example, the distributed-element counterpart of a five-element Chebyshev filter with 0.1 dB ripple was derived. The lumped-element filter and its calculated input reflectance data are given in Fig. 3 and Table 2, respectively.

An alternative transformation applicable to the design of distributed-element Chebyshev filters was proposed in [15,16]. A major drawback of this approach, however, is the deviation of the synthesized transducer power gain within the passband from that of the lumped-element filter. This is in contrast to our approach, where the transfer characteristic is preserved over the entire specified frequency band (see Figs. 5 and 7).

After selecting $n=6$, $n_\lambda=6$ and $k=0$, the polynomial $f(\lambda)$ was constructed as $f(\lambda)=(1-\lambda^2)^{6/2}=-\lambda^6+3\lambda^4-3\lambda^2+1$. Then, $S_{11}(\lambda)$ was generated as $S_{11}(\lambda)=h(\lambda)/g(\lambda)$, where

$$h(\lambda) = -10.4086\lambda^6 - 3.26\lambda^5 - 11.8448\lambda^4 - 3.3336\lambda^3 - 2.2268\lambda^2 - 0.7053\lambda \quad (15)$$

and

$$g(\lambda) = 10.4565\lambda^6 + 23.1667\lambda^5 + 36.6585\lambda^4 + 34.2382\lambda^3 + 20.3094\lambda^2 + 6.8641\lambda + 1. \quad (16)$$

The reflection coefficient $S_{11}(\lambda)$ was synthesized by using Richard's extraction [9]. In the next step, the desired distributed-element Chebyshev filter model with the characteristic impedances Z_i was obtained, as illustrated by Fig. 4. The delay τ can be obtained as usual from the length l of the distributed element and the phase velocity c : $\tau=l/c$.

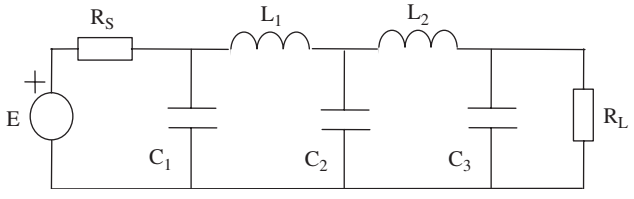

Fig. 3. Lumped-element low-pass Chebyshev filter with 0.1 dB ripple (normalized element values: $R_S=R_L=1$, $L_1=L_2=1.3712$, $C_1=C_3=1.1468$, $C_2=1.9750$) [14].

If l is chosen as a fraction $1/K$ of the wavelength $\Lambda=c/f_m$, it follows that $\tau=2\pi/K\omega_m$. To provide a safe limit for the end of the stop band, a scaled frequency γf_m, $\gamma>1$, may be advantageous [9]. In the design, $K=4$, $\gamma=1.1$, and $\omega_m=0.9$ were chosen (Table 2), eventually leading to a normalized value of $\tau=0.7933$.

Fig. 5 displays a comparison of the transducer power gain for the ideal lumped-element filter and the resulting distributed-element version. The close matching of the two curves illustrates that the distributed-element model presents a satisfactory counterpart of the given lumped-element low-pass Chebyshev filter.

In a next step, the cutoff frequency was selected as $f_m=1$ GHz, allowing the components of the designed distributed-element Chebyshev filter to be de-normalized. The appropriate lengths and widths of the distributed elements were computed by using the LineCalc program of ADS [17], with the results summarized in Table 3.

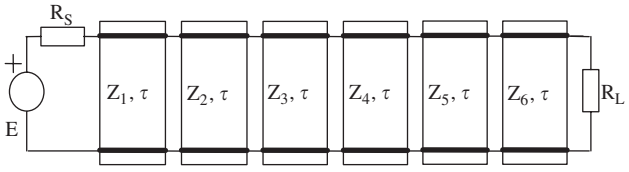

Fig. 4. Distributed-element Chebyshev filter (normalized element values: $R_S=R_L=1$, $Z_1=0.6125$, $Z_2=1.5597$, $Z_3=0.4625$, $Z_4=1.6564$, $Z_5=0.5680$, $Z_6=1.2997$, $\tau=0.7933$).

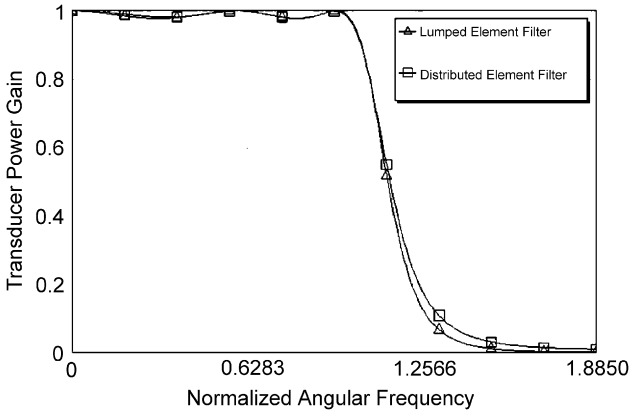

Fig. 5. Comparison between model and calculated data.

Table 2. Calculated input reflection data for the lumped-element Chebyshev filter with 0.1 dB ripple

Normalized frequency ω_i	0	0.1	0.2	0.3	0.4	0.5	0.6	0.7	0.8	0.9
Re$\{S(j\omega_i)\}$	0	−0.025	−0.082	−0.130	−0.131	−0.075	0.0096	0.0551	0.209	−0.032
Im$\{S(j\omega_i)\}$	0	−0.069	−0.098	−0.076	−0.023	0.0150	−0.006	−0.086	−0.149	−0.091

Table 3. Widths and lengths of the distributed elements

	Z_1	Z_2	Z_3	Z_4	Z_5	Z_6
Impedance (Ω)	30.6242	77.9855	23.1267	82.8195	28.4021	64.9835
Width (mm)	2.62	0.61	3.7	0.54	2.87	0.85
Length (mm)	22.5352	23.8795	22.2174	23.978	22.4457	23.5864

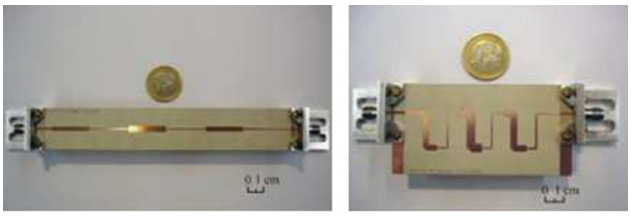

(a) (b)

Fig. 6. Fabricated distributed-element filters (a) with straight lines and (b) with bended lines.

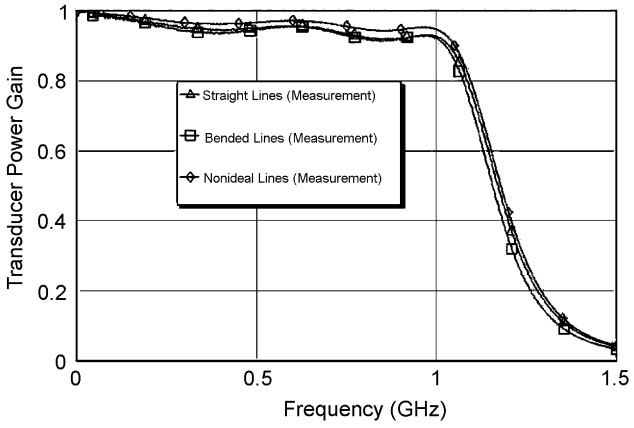

Fig. 7. Transducer power gain curves of the fabricated filters.

Finally, the filter was fabricated according to these design values using copper plated Rogers R03203 substrates (dielectric permittivity $\varepsilon_r = 3.02$, dielectric loss tangent Tan $\delta = 0.0016$, metal conductivity $\kappa = 5.8e7$ S/m, dielectric thickness $H = 0.508$ mm, and metallization thickness $T = 17$ μm). Fig. 6 shows the photographs of two versions of the fabricated filter. In Fig. 6a, the distributed elements are laid out as straight lines, while in Fig. 6b the elements are bent, to reduce the size of the filter. The occupied areas of the filter are $15.8\,\text{cm} * 2.5\,\text{cm} = 39.5\,\text{cm}^2$ and $7.6\,\text{cm} * 3.9\,\text{cm} = 29.64\,\text{cm}^2$ in Figs. 6a and 6b, respectively.

The measured transducer power gain of the two filters is displayed in Fig. 7 (triangles and squares). Both versions showed virtually undistinguishable performance. For comparison, the computed transducer power gain of the denormalized distributed-element filter is shown (diamonds). In order to account for the unavoidable dissipation losses in the transmission line elements, the geometry of the ideal (i.e., lossless) filter elements had been accordingly adapted by conventional CAD tools.

4. Conclusion

A reflectance-based tool was presented, to model the measured data obtained from a lumped-element network by means of its Darlington equivalent. Unlike other techniques, the proposed method does not require any choice of circuit topology nor complex cascade blocks; the elementary structure of the circuit is the natural consequence of the new modeling tool. The modeling algorithm and the related iteration procedure were described in detail. As an application example, a distributed-element Chebyshev filter was modeled, designed, fabricated, and successfully experimentally verified. Excellent agreement between simulated and measured transducer power gain were observed within passband and stopband.

The new distributed-element modeling tool enhances the analysis, design, and simulation capabilities of commercially available CAD tools, to manufacture distributed-element networks for high-speed, high-frequency analog/digital communication systems.

Acknowledgments

One author (MŞ) acknowledges support by the Scientific and Technical Research Council of Turkey (TUBITAK), Scientific Human Resources Development (BIDEB). This research has been conducted in part within the NEWCOM Network-of-Excellence in Wireless Communications funded through the EC 6th Framework Programme and Istanbul University Research Fund UDP-964/18042007. The authors would like to thank the reviewer who spent considerable amount of time reviewing the paper and providing excellent comments.

References

[1] Smilen LI. Interpolation on the real frequency axis. IEEE Int Conv Rev 1965;13(7):42–50.
[2] Zeheb E, Lempel A. Interpolation in the network sense. IEEE Trans Circuit Theory 1966;13(1):118–9.
[3] Youla DC, Saito M. Interpolation with positive real functions. J. Franklin Inst 1948; 217–20.
[4] Richards PI. Resistor transmission line circuits. Proc IRE 1967;284(2):77–108.
[5] Belevitch V. Classical network theory. San Francisco, CA: Holden Day; 1968.

[6] Aksen A. Design of lossless two-port with mixed, lumped and distributed elements for broadband matching. Dissertation. Ruhr University, Bochum, 1994.
[7] Ikeno N. A design theory of distributed constant filters. J Electron Commun Eng Japan 1952;35:544–9.
[8] Carlin HJ, Friedenson RA. Gain bandwidth properties of a distributed parameter load. IEEE Trans Circuit Theory 1968;15:455–64.
[9] Carlin HJ. Distributed circuit design with transmission line elements. Proc IEEE 1971;3:1059–81.
[10] Fettweis A. Cascade synthesis of lossless two ports by transfer matrix factorization. In: Boite R, editor. Network theory. London: Gordon & Breach; 1972.
[11] Yarman BS, Kılınç A, Aksen A. Immitance data modeling via linear interpolation techniques: a classical circuit theory approach. Int J Circuit Theory Appl 2004;32(6):537–63.
[12] Yarman BS, Şengül M, Kılınç A. Design of practical matching networks with lumped elements via modeling. IEEE Trans Circuits Syst I, Reg Papers, submitted.
[13] Burden RL, Faires JD. Numerical analysis. 7th ed., Thomson Learning: Brooks/Cole; 2001.
[14] Hong JS, Lancaster MJ. Microstrip filters for rf/microwave applications. New York: Wiley Series in Microwave and Optical Engineering; 2001.
[15] Rhodes JD. Design formulas for stepped impedance distributed and digital wave maximally flat and chebyshev low-pass prototype filters. IEEE Trans CAS 1975;22(11): 866–74.
[16] Carlin HJ, Civalleri P. Wideband circuit design. Boca Raton, FL: CRC Press LLC; 1998.
[17] Advanced Design Systems (ADS) of Agilent Techologies. ⟨www.home.agilent.com⟩.

Metin Şengül, received B.Sc. and M.Sc. degrees in Electronics Engineering from İstanbul University, Turkey, in 1996 and 1999, respectively. He completed his Ph.D. in 2006 at Işık University, İstanbul, Turkey. He worked as a technician at İstanbul University from 1990 to 1997. He was a circuit design engineer at R&D Labs of the Prime Ministry Office of Turkey between 1997 and 2000. Since 2000, he is a lecturer at Kadir Has University, İstanbul, Turkey. Currently he is working on microwave matching networks/amplifiers, data modeling and circuit design via modeling. Dr. Şengül is a visiting researcher at Institute for Information Technology, *Technische Universität Ilmenau*, Ilmenau, Germany.

Sıddık B. Yarman, B.Sc. in Electrical Engineering (EE), İstanbul Technical University (ITU), İstanbul, Turkey, 1974; MEEE in Electro-Math Stevens Institute of Technology (SIT) Hoboken, NJ., 1977; Ph.D. in EE-Math Cornell University, Ithaca, NY, 1982. Member of the Technical Staff (MTS) at Microwave Technology Centre, RCA David Sarnoff Research Center, Princeton, NJ (1982–1984). Associate Professor, Anadolu University, Eskişehir, Turkey, and Middle East Technical University, Ankara, Turkey (1985–1987). Visiting Professor and Research Fellow of Alexander Von Humboldt, Ruhr University, Bochum, Germany (1987–1994). Founding Technical Director and Vice President of STFA Defense Electronic Corp. İstanbul, Turkey (1986–1996). Full Professor, Chair of Division of Electronics, Chair of Defense Electronics, Director of Technology and Science School, İstanbul University (1990–1996). Founding President of Işık University, İstanbul, Turkey (1996–2004). Chief Advisor in Charge of Electronic and Technical Security Affairs to the Prime Ministry Office of Turkey (1996–2000). Chairman of the Science Commission in charge of the development of the Turkish Rail Road Systems of Ministry of Transportation (2004). Member Academy of Science of New York (1994), Fellow of IEEE (2004). Prof. Yarman has been back to İstanbul University since October 2004 and spending his sabbatical year of 2006–2007 at Tokyo Institute of Technology, Tokyo, Japan.

Christian Volmer, born in Düsseldorf, Germany, in 1980, received the Dipl. Ing. degree in Electrical Engineering and Information Technology from the *Technische Universität Ilmenau* in 2005. He is currently working there towards his doctorate at the Department of RF & Microwave Techniques. His present research activities concentrate on the application of miniaturized adaptive antenna arrays to mobile satellite communications. He conducts a research project funded by the German Ministry for Education and Research.

Matthias A. Hein, received his Diploma and Doctoral Degree in Experimental Physics from the University of Wuppertal in 1987 and 1992, respectively. For his work on satellite-based navigation systems in the framework of the US Navy's HTSSE project, he received the Alan Berman Research Publication Award. Since 1992, he has conducted interdisciplinary research on passive superconducting microwave electronics and materials, and completed his *Habilitation* in 1998. He was with the University of Birmingham (Great Britain) as an EPSRC Senior Research Fellow in 1999/2000. In 2002, he joined the Faculty of Electrical Engineering and Information Technology at the *Technische Universität Ilmenau* as a professor. Heading the Department for RF & Microwave Techniques, his present research interests cover novel microwave concepts and materials for various applications, including wireless communications and sensor technology. He has been invited to numerous international workshops and summer schools, authored and co-authored various monographs, reviews, and about 190 technical papers, and supervised about 40 Diploma and Doctoral students.